

Technical Note

Development and evaluation of a Perspex anthropomorphic head and neck phantom for three dimensional conformal radiation therapy (3D-CRT)

Khaldoon M. Radaideh^{1,2}, Laila M. Matalqah^{3,4}, A. A. Tajuddin^{5,2}, W. I. Fabian Lee⁶, S. Bauk⁷, E. M. Eid Abdel Munem²

¹*School of Medical Imaging and Radiotherapy, Allianze University College of Medical Sciences (AUCMS), Kepala Batas, Penang, Malaysia,* ²*School of Physics, Universiti Sains Malaysia, Penang, Malaysia,* ³*School of Pharmaceutical Sciences, Universiti Sains Malaysia, Penang, Malaysia,* ⁴*School of Pharmacy, Allianze University College of Medical Sciences (AUCMS), Kepala Batas, Penang, Malaysia,* ⁵*Advanced Medical and Dental Institute, Universiti Sains Malaysia, Kepala Batas, Penang, Malaysia,* ⁶*Department of Radiotherapy and Oncology, Mount Miriam Cancer Hospital, Jalan Bulan, Penang, Malaysia,* ⁷*Physics Section, School of Distance Education, Universiti Sains Malaysia, Minden, Penang, Malaysia*

(Received 6th May 2012; revised 11th May 2012; accepted 14th May 2012)

Abstract

Purposes: To design, construct and evaluate an anthropomorphic head and neck phantom for the dosimetric evaluation of 3D-conformal radiotherapy (3D-CRT) dose planning and delivery, for protocols developed by the Radiation Therapy Oncology Group (RTOG).

Materials and methods: An anthropomorphic head and neck phantom was designed and fabricated using Perspex material with delineated planning target volumes (PTVs) and organs at risk (OARs) regions. The phantom was imaged, planned and irradiated conformally by a 3D-CRT plan. Dosimetry within the phantom was assessed using thermoluminescent dosimeters (TLDs). The reproducibility of phantoms and TLD readings were checked by three repeated identical irradiations. Subsequent three clinical 3D-CRT plans for nasopharyngeal patients have been verified using the phantom. Measured doses from each dosimeter were compared with those acquired from the treatment planning system (TPS).

Results: Phantom's measured doses were reproducible with <3.5% standard deviation between the three TLDs' repeated measurements. Verification of three head and neck 3D-CRT patients' plans was implemented, and good agreement between measured values and those predicted by TPS was found. The percentage dose difference for TLD readings matched those corresponding to the calculated dose to within 4%.

Conclusion: The good agreement between predicted and measured dose shows that the phantom is a useful and efficient tool for 3D-CRT technique dosimetric verification.

Keywords: anthropomorphic head and neck Phantom; 3D-CRT; thermoluminescent dosimeter

INTRODUCTION

Nasopharyngeal cancer (NPC) is the third most common cancer among Malaysian men. In 2006, there were a total of 981 NPC cases registered in the Malaysian National Cancer Registry.¹ NPC is a challenging site for treatment with intensity-modulated radiation therapy (IMRT),² with the advantage of parotid glands sparing as compared with conventional 3D-conformal radiotherapy technique (3D-CRT) in terms of clinical outcome.³ However, 3D-CRT is still an acceptable treatment modality in resource-scarce community, as it offers comparable survival rates, locoregional control and metastasis-free survival, as compared with IMRT.⁴ 3D-CRT technique relies significantly on the planner's expertise, and such plans require effort in manipulation to achieve optimal dose distribution. In addition to that, the complexity of clinical treatment planning and treatment planning systems (TPS) by 3D-CRT have led to the need for a continuous quality assurance tests that can be applied to clinical treatment planning.⁵

Verification of the patient's plan before treatment is the standard of radiotherapy practice. This might achieve the validation of both data transferred and intended dose delivered, as computer TPS has many possibilities of dosimetric errors between planned and delivered treatments from the first step of the simulation process to the execution of treatment, and it also depends on the accuracy of the input dosimetry data using a certain protocol. The ultimate check of the actual dose delivered to a patient in radiotherapy can then be achieved by dosimetric measurement. This is perhaps the most accurate, obvious way to check the accuracy of patient treatment and to assess the delivered dose to critical organs or in difficult geometries where the dose is hard to predict from the treatment plan. Dosimetry can also be used to monitor the dose delivery in special treatment techniques. Therefore, there is a scope of dosimetric study that enhances dose verification in radiotherapy, thus providing options to minimise the possible errors in dose delivery.

Phantom made up of a material approximating soft tissue is highly recommended by the American Association of Physics in Medicine,

Radiation Therapy Committee (AAPM-RTC). It is to be used in assessing the patient contour accurately and verify at the same time the (3D-CRT) techniques at both the commissioning and clinical stages. It should also provide a realistic representation of the clinical site being treated. Ideally, these phantoms should be anatomically realistic, have radiologic properties that are identical to the tissues concerned and allow for a variety of measuring devices to be used to verify dose and its distribution in a number of key positions throughout the target and normal tissue volumes.⁶ An anthropomorphic head and neck phantom made up of material approximating soft tissue had been used in previous studies.^{7,8} The availability and the similarity of that material's density⁸ to the average density of tissues and bones in the human head and neck regions must be considered when choosing Perspex as the material for fabricating the current phantom.

In previous literatures, a head and neck phantom was designed with plastic shell filled with water for dosimetric validation of IMRT. thermoluminescent dosimeters (TLDs) and radiochromic films were used to measure the absolute dose and the dose distribution in two Planning Target Volume (PTV) and Organ at risk (OAR) areas. The insert was constructed as a block of polystyrene-housing solid water targets and an acrylic OAR. Only one OAR was considered located in one area.⁹ Another semi-anatomic phantom of head and neck region using Perspex material was designed and intended mainly for the verification of IMRT treatments in the head and neck region.⁷ Semnicka et al.⁸ also designed a dedicated glass phantom used to investigate the possibility of implanting real bone samples and bone substitutes into a gel sample. Attention was paid to the head and neck treatment verification as this location presents a complex site with irregular surface and different heterogeneous organs (e.g. spinal cord, vertebrae, larynx, etc.). However, this phantom was not involved in dosimetric verification studies. A summary of designed head and neck phantoms is shown in Table 1.

The goal of this study is to establish a method for taking in-phantom measurements of organ

Table 1. Summary of some designed head and neck phantoms' characteristics and applications

References	Phantom material	Characteristics	Using in dosimetry	Dosimeters used	OAR regions	PTV
Molineu et al. (2005)	Plastic filled with water	Head-shaped shell	Evaluation of IMRT	TLDs and radiochromic film	1	Yes
Webster et al. (2008)	Perspex	Semi-anatomic phantom for head and neck	Verification for IMRT	Thimble ionization chamber (0.125 cm ³ : PTW, Freiburg, Germany) PinPoint chamber (0.015 cm ³ : PTW)	None	Yes
Šemnická. J (2009)	Glass, polyacrylamide gel (PAG)	A dedicated glass phantom for head and neck regions supplied with vertebra or its substitutes	Quantifying the absorbed dose in the spine Quantifying imaging artefact by MRI scanning	None	None	No
Present study	Perspex	Anatomic phantom for head and neck	Design phantom for 3D-CRT dosimetric verification	Thermoluminescent dosimeters (TLDs)	8	Yes

doses for out-of-field photon exposures, resulting from selected typical 3D-CRT treatment plan. The present paper details the considerations involved in the design, construction, development and evaluation of Perspex anthropomorphic phantom for 3D-CRT dose delivered to the PTVs and OARs in NPC patients' treatment plans.

MATERIALS AND METHODS

Phantom design and development

In designing the phantom, attention was paid to the adequate representation of dose distribution and the standardisation of our phantom size and contouring (Figure 1). Computed tomography (CT) images for series of nasopharyngeal patients using SIEMENS CT Scanner (SOMATOM Sensation Open, Germany) were obtained and transferred to TPS. In collaboration with a group of physicists, the dimensions of the head and neck regions were obtained and the average was considered. The primary and secondary PTVs and OARs were delineated in collaboration with a group of medical physicists and a radiologist, and print out of transverse sections were obtained. By matching and contouring the images of the printed CT scan slices on Perspex boards, 39 slices of Perspex were cut so that when assembled they could represent the model of a patient's head and neck region (Figure 2). Two perpendicular isocentre lines on printed CT images were determined on the Perspex for each slide to

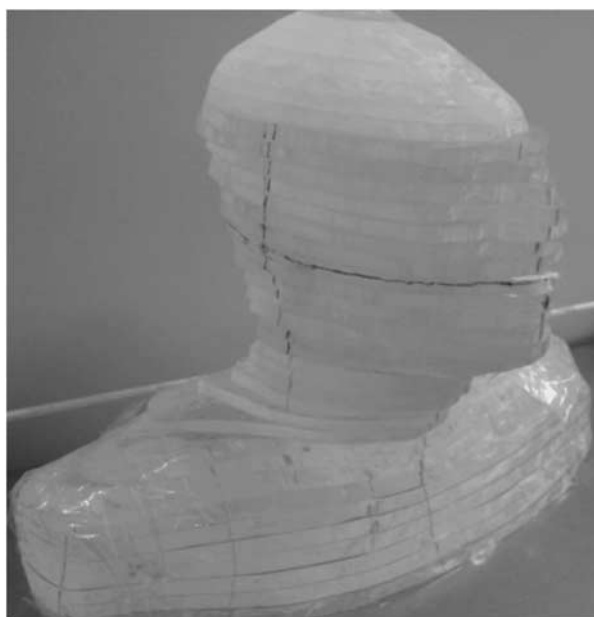
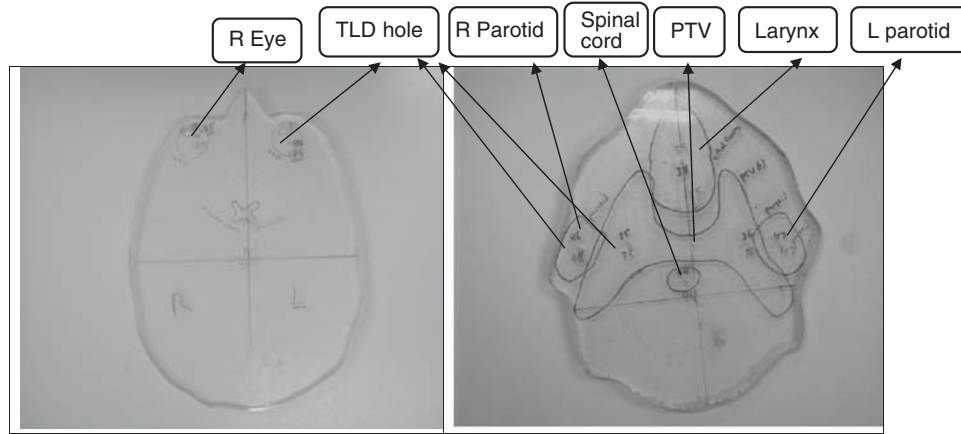


Figure 1. Anatomical Perspex head and neck phantom for the verification of treatment delivery.

make it easy to build according to these lines. Eight OARs were selected, including eyes (bilateral), parotid glands (bilateral), brain stem, optic chiasm, larynx and spinal cord, in addition to both sides of planning target volumes (PTV) that included the borderline. Ninety-four holes with the dimension of 1.5 mm (width) × 8 mm (depth) were drilled into various locations within OAR and PTV regions in each slide for the placement of TLDs. To avoid any influence on



Abbreviations: TLD = Thermoluminescent Dosimeter;
PTV= planning target volumes; R= right; L=Left.

Figure 2. Perspex slices with delineated organs at risk and planning target volume boundaries.

Abbreviations: TLD, thermoluminescent dosimeter; PTV, planning target volumes; R, right; L, left.

TLD dose because of the slightly higher density of the TLDs (2.64 g/cm^3),¹⁰ holes were drilled at least 1 cm apart. A CT scan was then performed on the fabricated phantom to acquire the transverse images to locate the position of the TLDs (Figure 3).

TLD calibration

Rod-shaped LiF:Mg, Ti TLDs, with dimensions of $1.0 \text{ mm diameter} \times 6.0 \text{ mm length}$, as obtained from the manufacturer (Bicron, NE, USA), were used in this study. As TLDs, as dosimeters, can be reused hundreds of times, annealing treatment should be done before each irradiation. This is required especially in medical therapy applications, where high doses are the norm and the highest accuracy is desired.^{11,12} In the present study, LiF:Mg,Ti TLDs were annealed by using a Nabertherm oven (Nabertherm, Germany) for 1 hour at 400°C , 2 hour cooling, followed by 24 hour at 80°C .^{11,13} All TLDs were selected after a careful initialisation procedure.¹⁴

For TLD calibration, solid water phantom was used to determine the percentage depth dose (PDD), by which a correction factor was found.¹⁵ As we did not wish to create holes in the solid water phantom to place the TLDs, a number of 4 mm thick slabs of Perspex were drilled with holes on the surface with dimensions of 1.5 mm



Figure 3. Anatomical Perspex head and neck phantom during CT scan.

(diameter) $\times 1.5 \text{ mm (depth)} \times 8 \text{ mm (length)}$. The slabs were inserted between the solid water phantom (Nuclear Associates, Chicago, IL, USA) at d_{max} . The 6 MV photon beam was used to irradiate the TLDs from a Siemens Mevatron MX2 linear accelerator (Siemens Inc., USA) used to irradiate TLDs at a nominal SSD of 100 cm with a $(10 \times 10 \text{ cm}^2)$ field size. All TLD readout was carried out by a Harshaw TLD reader model 3500 (Harshaw, USA). The reading profile was as follows: preheat temperature of 50°C for 0 second, acquire temperature rate 12°C/second , acquire maximum temperature of 300°C for $33\frac{1}{3}$ second and annealing temperature of 300°C for 0 second.

For calibration purposes, a dose of 100 cGy was delivered from 6-MV photon beam, and a FC65-G (Wellhofer, Germany) ionisation chamber was used. The accuracy of TLD measurements depends on the reproducibility of the results,^{13,14,16} as measured by the standard deviation of each individual calibration factor. Six subsequent calibration cycles were carried out to establish the individual calibration factors.

Percentage depth dose curve

A PDD curve study was conducted by exposing the TLDs and the ion chamber at different depths (ranging from 0 to 20 cm) and 10 cm thickness as full backscatter in the Solid Water Phantom at reference settings. The correction factor was obtained as the ratio of M_w and M_{pl} , where M_w is the average of five ion chamber readings at 1.5 cm in a water phantom and M_{pl} is the average of five TLD readings at the same depth in a Perspex phantom. All ion chamber readings were corrected for the water temperature and atmospheric pressure. For both set-ups, $D_0 = 100$ cGy was delivered at d_{max} .

Phantom's reproducibility test

In order to check the reproducibility as a phantom, a treatment plan was used. This plan was generated 2 Gy to at least 95% of the primary and 1.8 Gy to at least 95% of the secondary PTVs. Less than 1% of the primary and secondary PTVs should receive <93% of the prescription dose. OARs have to receive <1.5 Gy, and the normal tissue should not receive >110% of the primary PTV prescription dose, with dose constraints according to ROTG protocol.¹⁷ A total of 94 TLDs were placed in the holes within eight OAR and PTV regions and three fractions of 6-MV X-ray beam using two lateral fields and matched with lower anterior neck field (Figure 4). After each shot, TLDs were readout, annealed and then reinserted into phantom slices.

Phantom implementation on dosimetric verification of 3D-CRT

Three nasopharyngeal patients' treatment plans were chosen and carried out on the designed phantom by matching the isocentre using TPS



Figure 4. Anatomical Perspex head and neck phantom during 3D-CRT treatment.

(ONCENTRA MAHERPLAN V3.3). The delineation of OARs and PTVs was adjusted to insure that TLD holes are located inside the boundaries of OAR and PTV regions. After loading phantom with TLDs, it was irradiated three times for each plan. TLDs were read out and the average measurements were considered. Calculated point doses at corresponding points were obtained from TPS by pencil beam algorithm. The measured doses at each OAR were then compared with the constraints doses, according to Radiation Therapy Oncology Group (RTOG 0615).¹⁷

RESULTS AND DISCUSSION

The TLDs selected and used in dose verification should have been tested for reproducibility and dose response. All TLDs were calibrated in a primary beam of 6-MV photon. However, some measurements were taken outside the main field where the scattered photons had lower energy than the main energy. An energy correction factor of 1.04 for TLD-100 measurement was performed in the outfield.^{18,19} However, the energy response of TLD-100 to photon with energy higher than 1 MeV remained constant with negligible energy dependence.^{17,20} After TLDs were irradiated six times, the TLDs, whose reproducibility within 3% and sensitivity within 10%, were used in this study. In agreement with another study, where the standard deviations of TLD-100 reproducibility response was 3–5% to delivered doses ranging from 1 to 5 Gy,²¹ the

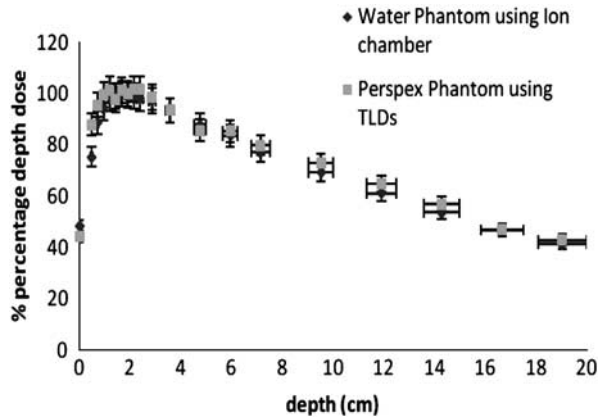


Figure 5. Central axis depth dose distribution for 6-MV photon beam at field size ($10 \times 10 \text{ cm}^2$), $\text{SSD} = 100 \text{ cm}$, using ion chamber in water Phantom and TLDs in Perspex Phantom. Abbreviation: TLDs, thermoluminescent dosimeters.

TLDs displayed a linear response ($R^2 = 0.998$) with respect to the measured doses at d_{max} ranging from 0.5 to 4 Gy. No energy correction factors were used as the reproducibility of our TLDs that had a standard deviation of $<3\%$.

Phantom material can be a source of error during dosimetric measurements. Therefore, a correction factor ($K_{\text{correction}}$) for Perspex material should be considered. In previous literature, the correction factor at 6-MV was found about 1.068 using TLDs and 1.063 using Monte Carlo simulation²² and it was 1.0500 ± 0.0003 in this study. This correction replaces all corrections for sensitivity, phantom material, field size and fading. By multiplying the absorbed dose measured by the TLDs in the Perspex phantom with the dose correction factor, the absorbed dose to water at the calibration depth can be obtained. The PDD curves using TLDs in Perspex phantom and ion chamber in water phantom are presented in Figure 5.

To determine how well the phantom's results could be reproduced, treatment plan for the phantom was designed and delivered three times identically. Data entry and analyses were carried out by Excel and SPSS software version 17.0 (statistical package of social sciences) (SPSS Inc., Chicago, IL, USA) programs. The average point-by-point percent standard deviation between the three TLD readings at identical settings was

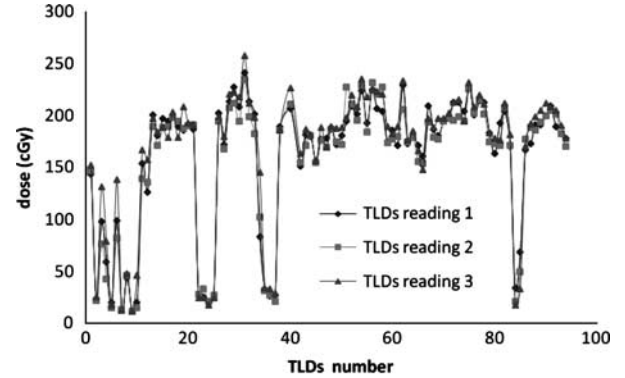


Figure 6. TLD reading for three identical irradiations, measured in cGy.

Abbreviation: TLDs, thermoluminescent dosimeters.

$<3.5\%$ (Figure 6). Hence, the TLD-100 in this study is usable in clinical dose verification. Furthermore, the dose discrepancies between the average of the three TLD readings and TPS were found to be $<4\%$ (Figure 7).

The applicability of the phantom in predicting the doses at eight clinical organs of interest was also studied. For three identical fractions, the average of TLD reading at each OAR was computed and compared with its corresponding calculated doses as obtained from TPS uses pencil beam algorithm (Table 2). There was a close relationship between the average measured and calculated doses with a mean correlation of 0.985, and standard deviations of 3.2% and 4% at OAR and PTV regions, respectively. In our centre, we set our acceptance criteria as 5% at high-dose regions (PTV) and 10% at low-dose regions (OAR) for dose verification in a phantom with ion chambers, TLD and MOSFET. An important source of errors in TPS is the dose computation of each spot to obtain the truly optimum final dose distribution. Inaccuracies in the spot dose distributions inevitably lead to systematic errors in the spot weights and may even be amplified in the optimisation.²³

In the anthropomorphic phantoms, there was a small air gap between each of the slabs of the phantom, which could not be completely eliminated. This is mainly developed because of the size differences between the holes and TLDs that was made slightly bigger to avoid TLD's scratching or breaking when assembling and constructing slices

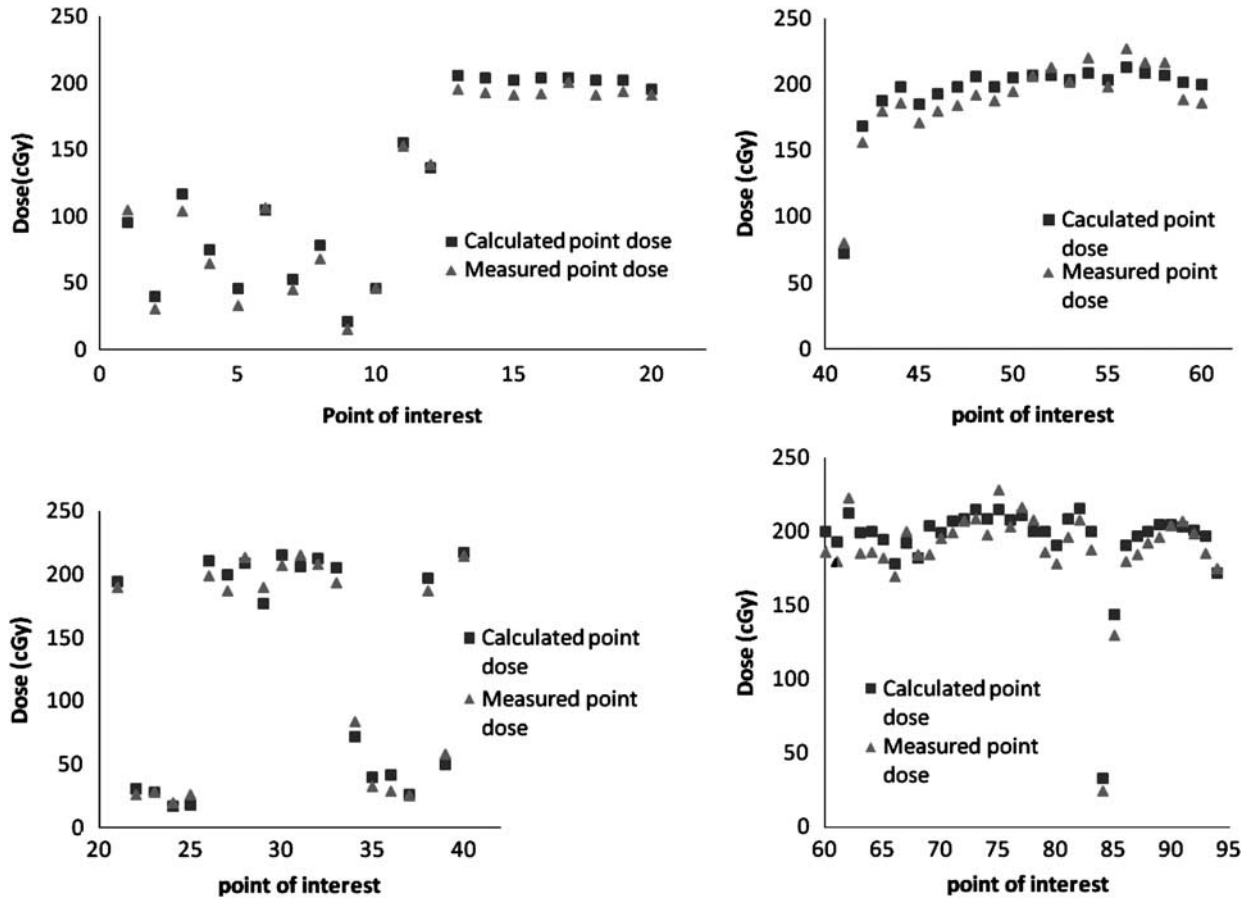


Figure 7. Comparison of average TLD measurements (cGy) and 3D-CRT treatment planning calculated doses for the dose verification.

Table 2. The average of three delivered doses at different OAR regions using phantom's plan in comparison with Radiation Therapy Oncology Group Protocol (RTOG 0615)

Organ at risk	No. of TLDs	Dose constraints (Gy)	Plan 1 (average of three shots)			
			$M_{av} \pm SD$ (cG)	M_{av} (Gy)	TPS (Gy)	Dose difference (%)
Optic chiasm	3	<54 Gy	85 ± 3.2	29.75	23.625	25.93
R eye	4	<45 Gy	47 ± 2.6	16.45	22.61	-27.24
L eye	4	<45 Gy	46.6 ± 3.9	16.31	22.435	-27.30
L parotid	4	<26 Gy	188 ± 4.4	65.8	71.435	-7.89
R parotid	4	<26Gy	193 ± 2.4	67.55	70.98	-4.83
Brainstem	4	<54 Gy	24.9 ± 2.5	8.715	8.12	7.33
Larynx	16	<45 Gy	166 ± 4.4	58.1	51.38	13.08
Spinal cord	13	<45 Gy	156 ± 2.0	54.6	58.38	-6.47
PTV 70	42	≥ 70 Gy	190 ± 4.0	66.5	69.72	-4.62
Mean						-3.56
SD (%)						17.39

Abbreviations: TLD, thermoluminescent dosimeter; TLDs, number of TLD; M_{av} (Gy), average measurement doses in Gy using TLD; TPS(Gy), calculated doses using treatment planning system; R, right; L, left.

to build the model. These air gaps could result in increased exposure to the TLDs owing to the decreased amount of attenuation present and lead to such dose discrepancies.

The total delivered doses at each OAR region in comparison with the constraints doses at critical normal structure as recommended by Radiation Therapy Oncology Group Protocol

Table 3. Dosimetric verification of three nasopharyngeal patients' treatment plans (3DCRT) using head and neck phantom

Organ at risk	No. of TLDs	Dose constraints	Plan 1			Plan 2			Plan 3		
			M _{av} (Gy)	TPS (Gy)	Dose difference (%)	M _{av} (Gy)	TPS (Gy)	Dose difference (%)	M _{av} (Gy)	TPS (Gy)	Dose difference (%)
Optic chiasm	3	<54 Gy	26.4	27.8	-5.0	35.2	38.3	-8.1	40.3	44.2	-8.8
R eye	4	<45 Gy	28.9	23.2	24.5	15.7	18.4	-14.7	29.2	33.5	-12.8
L eye	4	<45 Gy	16.2	22.4	-27.7	22.3	24.6	-9.3	18.4	20.4	-9.8
L parotid	4	<26 Gy	50.2	54.1	-7.2	37.5	39.1	-4.1	24.9	27.3	-8.8
R parotid	4	<26 Gy	45.2	39.4	14.7	32.7	30.2	8.3	23.5	27.3	-13.9
Brainstem	4	<54 Gy	25.3	28.4	-10.9	25.8	29.2	-11.6	33.2	31.5	5.4
Larynx	16	<45 Gy	50.5	56.3	-10.3	54.7	53.7	1.9	47.5	53.2	-10.7
spinal cord	13	<45 Gy	52.8	58.3	-9.4	53.9	56.8	-5.2	42.5	44.3	-4.1
PTV 70	51	≥ 70 Gy	66.1	70.4	-6.1	66.4	69.9	-5.0	68.8	70.5	-2.4
Mean					-4.2			-5.3			-7.3
SD (%)					15.2			7.0			6.0

Abbreviations: TLD, thermoluminescent dosimeter; TLDs, number of TLD; M_{av} (Gy), average measurement doses in Gy using TLD; TPS(Gy), calculated doses using treatment planning system; R, right; L, left.

(RTOG 0615)¹⁷ are shown in Table 2. For 3D-CRT plan, the doses were obviously above the constraint doses in three regions: parotid gland, larynx and the spinal cord. The functional changes of the parotid glands depend on the radiation dose and the irradiated volume²⁴ and it could be avoided until a dose <26 Gy.^{3,25-29}

Subsequent verification of three clinical head and neck 3D-CRT plans demonstrated the efficacy of the phantom in making a range of patient-specific dose measurements in regions of dosimetric and clinical interest. Agreement between measured values and those predicted by the TPS system was found to be generally accepted, with a mean error on the calculated dose to each point of -5.6% (range: -7.3% to -4.2%; $n = 3$) for all regions (Table 3).

CONCLUSION

This is a new handmade design of anthropomorphic head and neck phantom intended for dosimetric verification of 3D-CRT plans. It was designed with movable slices with delineated clinical organs and allow for the variety of measuring devices to be used, which enable the prediction of delivered doses at any organ of interest. The phantom's results have a preliminary, proved to be a valuable tool in the development and implementation of clinical head and neck 3D-CRT, allowing for the verification of absolute

dose in regions of clinical and dosimetric interest. Implementation of this phantom in IMRT plan verification would be considered in future work. Further modifications as finishing and holding technique will also be considered.

Acknowledgement

The paper is a part of the research conducted within the project (FRGS), number 203/PFIZIK/6711178, Universiti Sains Malaysia (USM), Penang Malaysia. The authors thank all radiologists, physicists and radiographers in the Radiotherapy Department of the Mount Miriam Cancer Center in Penang state, Malaysia for their cooperation and help.

References

- Omar Z, Mohd Ali Z, Ibrahim Tamin NS. Malaysian cancer statistics-data and figure Peninsular Malaysia, 2006.
- Kam M K M, Chau R, Suen J, Choi P H K, Teo P M L. Intensity-modulated radiotherapy in nasopharyngeal carcinoma: dosimetric advantage over conventional plans and feasibility of dose escalation* 1. *Int J Radiat Oncol Biol Phys* 2003; 56 (1): 145-157.
- Nutting C M, Morden J P, Harrington K J et al. Parotid-sparing intensity modulated versus conventional radiotherapy in head and neck cancer (PARSPORT): a phase 3 multi-centre randomised controlled trial. *Lancet Oncol* 2011; 12: 127-136.

4. Fang F M, Chien C Y, Tsai W L et al. Quality of life and survival outcome for patients with nasopharyngeal carcinoma receiving three-dimensional conformal radiotherapy vs. intensity-modulated radiotherapy – a longitudinal study. *Int J Radiat Oncol Biol Phys* 2008; 72 (2): 356–364.
5. Boyer A L, Mok E, Luxton G et al. Quality assurance for treatment planning dose delivery by 3DRTP and IMRT. In: Shiu A S, Mellenberg D E (eds). *General Practice of Radiation Oncology Physics in the 21st Century*. Madison, WI: Med Phys, Publishing, 2000: 187–230.
6. International Commission on Radiation Units and Measurements. *Tissue Substitutes in Radiation Dosimetry and Measurement*. Report 44, Bethesda, MD: ICRU, 1989.
7. Webster G J. Design and implementation of a head & neck phantom (HANK) for system audit and verification of IMRT. *J Appl Clin Med Phys* 2008; 9 (2): 2740.
8. Šemnická J, Váček V S, Veselský T, Koněk O. Designing phantom for head-and-neck treatment verification: Feasibility tests with bone and bone equivalent material incorporated into polymer gel. *J Phys, conference series* 164, 2009.
9. Molineu A, Followill D S, Balter P A et al. Design and implementation of an anthropomorphic quality assurance phantom for intensity-modulated radiation therapy for the Radiation Therapy Oncology Group. *Int J Radiat Oncol Biol Phys* 2005; 63 (2): 577–583.
10. Attix F. *Introduction to Radiological Physics and Radiation Dosimetry*, 1st edition. Wiley-VCH: Wiley Inter-science, 1986.
11. Horowitz Y S. *Thermoluminescence and Thermoluminescent Dosimetry*, v. 1, 1984.
12. McKinlay A. *Thermoluminescence Dosimetry*. Bristol: Hilger, 1981.
13. McKeever S W S, Moscovitch M, Townsend P D. *Thermoluminescence Dosimetry Materials: Properties and Uses*. Ashford, Kent: Nuclear Technology Publishing, Cambridge University Press, 1995.
14. Furetta C, Weng P S. *Operational Thermoluminescence Dosimetry*. Singapore: World Scientific Pub Co Inc, 1998.
15. Radaideh K, Alzoubi A. Factors impacting the dose at maximum depth dose (d_{max}) for 6 MV high-energy photon beams using different dosimetric detectors. *Biohealth Sc Bulletin* 2010; 2 (2): 38–42.
16. Yazici N. The influence of heating rate on the TL response of the main glow peaks 5 and 4+ 5 of sensitized TLD-100 treated by two different annealing protocols. *Nuclear Instruments and Methods in Physics Research Section B: Beam Interactions with Materials and Atoms* 2004; 215 (1–2): 174–180.
17. Lee N, Pfister D, Garden A. RTOG 0615, A phase II study of concurrent chemoradiotherapy using three-dimensional conformal radiotherapy (3D-CRT) or intensity-modulated radiation therapy (IMRT)+ bevacizumab (BV) for locally or regionally advanced nasopharyngeal cancer, 2009.
18. Kry S F, Titt U, Pönisch F et al. A Monte Carlo model for calculating out-of-field dose from a Varian 6 MV beam. *Med Phys* 2006; 33 (11): 4405.
19. Charalambous S, Petridou C. The thermoluminescence behaviour of LiF (TLD-100) for doses up to 10 M Rad. *Nucl Instrum Methods* 1976; 137 (3): 441–444.
20. Kron T, Duggan L, Smith T et al. Dose response of various radiation detectors to synchrotron radiation. *Phys Med Biol* 1998; 43: 3235–3259.
21. Harris C K, Elson H R, Lamba M A S, Foster A E. A comparison of the effectiveness of thermoluminescent crystals LiF:Mg, Ti and LiF:Mg, Cu, P for clinical dosimeters. *Med Phys* 1997; 24 (9): 1527–1529.
22. Lee J, Yeh C, Hsueh S et al. Simple dose verification system for radiotherapy radiation. *Radiat Measurements* 2008; 43: 954–958.
23. Jeraj R, Keall P J, Siebers J V. The effect of dose calculation accuracy on inverse treatment planning. *Phys Med Biol* 2002; 47: 391–407.
24. Bekes K, Francke U, Schaller H G et al. The influence of different irradiation doses and desensitizer application on demineralization of human dentin. *Oral Oncol* 2009; 45 (9): e80–e84.
25. Vergeer M R, Doornaert P A H, Rietveld D H F, Leemans C R, Slotman B J, Langendijk J A. Intensity-modulated radiotherapy reduces radiation-induced morbidity and improves health-related quality of life: results of a nonrandomized prospective study using a standardized follow-up program. *Int J Radiat Oncol Biol Phys* 2009; 74 (1): 1–8.
26. Eisbruch A, Clifford C K S, Garden A. RTOG 0022: Phase I/II Study Of Conformal And Intensity Modulated Irradiation For Oropharyngeal Cancer Radiation Therapy Oncology Group, 2004.
27. Eisbruch A, Ship J A, Martel M K et al. Parotid gland sparing in patients undergoing bilateral head and neck irradiation: techniques and early results. *Int J Radiat Oncol Biol Phys* 1996; 36 (2): 469–480.
28. Malouf J G, Aragon C, Henson B S et al. Influence of parotid-sparing radiotherapy on xerostomia in head and neck cancer patients. *Cancer Detection and Prevention* 2003; 27 (4): 305–310.
29. Jabbari S, Kim H M, Feng M et al. Matched case-control study of quality of life and xerostomia after intensity-modulated radiotherapy or standard radiotherapy for head-and-neck cancer: initial report. *Int J Radiat Oncol Biol Phys* 2005; 63 (3): 725–731.